

Structure and Nonlinear Optical Properties of $\text{Sb}_2\text{O}_3\text{--B}_2\text{O}_3$ Binary GlassesKentaro TERASHIMA, Tadanori HASHIMOTO*, Takashi UCHINO,
Sae-Hoon KIM** and Toshinobu YOKO*Institute for Chemical Research, Kyoto University, Gokasho, Uji-shi, Kyoto 611***Department of Chemistry for Materials, Faculty of Engineering, Mie University, 1515, Kamihama-cho, Tsu-shi, Mie 514****Ceramic Materials Research Institute, Hanyang University, Seoul 133–791, Korea* $\text{Sb}_2\text{O}_3\text{--B}_2\text{O}_3$ 二成分系ガラスの構造と非線形光学特性

寺島健太郎・橋本忠範*・内野隆司・金 世勲**・横尾俊信

京都大学化学研究所, 611 京都府宇治市五ヶ庄

*三重大学工学部分子素材工学科, 514 三重県津市上浜町 1515

**漢陽大学セラミック素材研究所, 133-791 大韓民国 Seoul 特別市城東区杏堂洞

The third order nonlinear optical susceptibilities $\chi^{(3)}$ of $\text{Sb}_2\text{O}_3\text{--B}_2\text{O}_3$ binary glasses have been measured by the third harmonic generation (THG) method. The IR and Raman spectroscopic study reconfirmed that the structure of Sb_2O_3 glass is similar not to senarmonite but to valentinite which consists of double-chains of SbO_3 units. The formation of BO_4 units is much smaller for $\text{Sb}_2\text{O}_3\text{--B}_2\text{O}_3$ glasses than $\text{Bi}_2\text{O}_3\text{--B}_2\text{O}_3$ glasses at all compositions, which is ascribed to the covalent character of Sb–O bonds. It is also considered that Sb_2O_3 is present as SbO_3 trigonal units and participates in the glass network formation through the Sb–O–B bonds. The $\chi^{(3)}$ value increased monotonically with increasing Sb_2O_3 content up to 8.4×10^{-13} esu for Sb_2O_3 glass, which is about 30 times larger than SiO_2 glass. Modified Lines' linear relationship between $\chi^{(3)}$ and $(n_o^2 + 2)^3 \cdot (n_o^2 - 1) \cdot E_d / E_0^2$ was adopted to $\text{Sb}_2\text{O}_3\text{--B}_2\text{O}_3$ glasses. [Received February 21, 1996; Accepted August 6, 1996]

Key-words : Third harmonic generation, Senarmonite, Valentinite, Sb_2O_3 glass, Covalency, Modified Lines' relationship

1. Introduction

Recently, nonlinear optical processes have drawn special attention due to their inherent ultra-fast response time. The response time of nonlinear optical processes is of the order of femtosecond (10^{-15} s) because of the purely electronic relaxation from the excited states. The utilization of the nonlinear process is, therefore, thought to be requisite for developing ultra-high-speed optical switching devices. Among nonlinear optical properties, the third order nonlinear optical effects are especially important in isotropic media such as glass. In general, as suggested by Adair et al.,¹⁾ glasses which contain ions of high polarizability are expected to have large nonlinear optical properties. So far, nonlinear optical properties of glasses containing heavy metal cations (e.g., Tl^+ , Pb^{2+} , Bi^{3+} , etc.) have been extensively investigated by Hall et al.²⁾ Such glasses are found to have high nonlinear optical properties as expected from the high polarizabilities of heavy metal cations.^{3,4)} The third order nonlinear susceptibility $\chi^{(3)}$ increases with an increase of the total heavy metal oxide (HMO) content. That is, in order to enhance the $\chi^{(3)}$ it is required to prepare glasses with the HMO content as high as possible. From this point of view, B_2O_3 glass is a superior host matrix for HMO because it vitrifies up to very high HMO content. Very recently, we have studied nonlinear optical properties of $\text{PbO--B}_2\text{O}_3$ and $\text{Bi}_2\text{O}_3\text{--B}_2\text{O}_3$ binary glasses and found that the $\chi^{(3)}$ of these glasses increases rapidly with increasing HMO content.⁵⁾

For a similar reason, $\text{Sb}_2\text{O}_3\text{--B}_2\text{O}_3$ system is of interest, because it vitrifies in the whole composition region.⁶⁾ In this case, it is also of interest to know the local structure of Sb^{3+} ion in view of the structural role in glass formation. However, the study on the structure of $\text{Sb}_2\text{O}_3\text{--B}_2\text{O}_3$ glasses is limited^{6–9)} and only little is known about the relationship between the structure and properties of the $\text{Sb}_2\text{O}_3\text{--B}_2\text{O}_3$ glasses.

In this paper, we study the structure of the $\text{Sb}_2\text{O}_3\text{--B}_2\text{O}_3$

glasses using IR, Raman and ^{11}B MAS NMR spectroscopies for a better understanding of the nonlinear optical properties of the glasses. We also measure the third order nonlinear optical susceptibilities ($\chi^{(3)}$) by the third harmonic generation (THG) method. We then interpret nonlinear optical properties of this glass system in terms of the covalency of Sb–O, the optical band gap, and the bond orbital theory.

2. Experimental procedure

Reagent grade senarmonite Sb_2O_3 (Wako Pure Chem. Ind., Ltd., Osaka, Japan) and B_2O_3 (Nacalai Tesque, Inc., Kyoto, Japan) were used as raw materials. The batch compositions (mol%) of $\text{Sb}_2\text{O}_3\text{--B}_2\text{O}_3$ glasses are shown in Table 1. A 10 g batch of well mixed reagents was melted in a platinum crucible with a lid at 850–900°C for 15 min using an electric furnace. The glasses were obtained by pouring the melts onto a stainless plate and pressing by another one. To obtain Sb_2O_3 glass, however, the batch of Sb_2O_3 was melted in a sealed and evacuated silica ampoule with inner diameter 8 mm and wall thickness 1.2 mm at 750°C for 20 min, and then the ampoule was quenched rapidly using a freezing mixture (–11 °C) consisting of ice, ethanol and NaCl. Prior to use, the samples were stored in a desiccator to avoid moisture attack.

The reference orthorhombic Sb_2O_3 valentinite was prepared by heating Sb_2O_3 senarmonite at 650°C for 12h in the flowing N_2 gas. The prepared samples were identified by an X-ray diffraction analysis.

IR spectra were measured by a KBr pellet technique using a Shimadzu FT-IR model spectrophotometer (FTIR-8000 series) in the frequency range of 400–2000 cm^{-1} .

Raman spectra of the glasses were measured with a Nippon Bunko model JASCO NR-1000S Raman spectrophotometer using the 514.5 nm line of Ar^+ laser as the exciting beam. The laser power was adjusted to 200–250 mW. The light scattered at 90° passed through a double

Table 1. Linear and Nonlinear Optical Properties* of Sb_2O_3 - B_2O_3 Glasses

Composition	Density	T_w	T_{3w}	n_w	n_{3w}	E_g	E_d	E_0	R_M	V_M	I/I_{SiO_2}	l_c	$\chi^{(3)}$
/ mol%	/ $\text{g} \cdot \text{cm}^{-3}$	/ %	/ %			/ eV	/ eV	/ eV	/ $\text{cm}^3 \cdot \text{mol}^{-1}$	/ $\text{cm}^3 \cdot \text{mol}^{-1}$		/ μm	/ 10^{14} esu
$x\text{Sb}_2\text{O}_3 \cdot (100-x)\text{B}_2\text{O}_3$													
x=0	1.797	90.8	82.6	1.425	1.440	7.2	6.17	6.42	9.91	38.7	0.61	14.5	2.88
x=10	2.394	90.7	79.6	1.444	1.451	4.52	14.6	13.5	10.2	38.3	1.48	13.4	4.96
x=20	2.930	86.1	72.1	1.614	1.667	4.31	9.45	5.95	13.6	38.9	2.44	10.9	10.6
x=30	3.406	86.2	72.1	1.673	1.708	4.10	13.3	7.46	15.0	40.0	3.63	9.17	16.4
x=40	3.994	83.9	73.3	1.791	1.810	3.91	23.1	10.5	16.8	39.7	5.00	6.75	30.2
x=50	4.369	86.1	74.3	1.840	1.865	3.76	22.9	9.64	18.3	41.3	5.51	6.21	35.6
x=60	4.474	81.2	77.7	1.881	1.895	3.74	33.0	13.0	20.8	45.3	6.53	5.89	44.0
x=70	4.713	85.6	77.7	1.908	1.922	3.60	33.7	12.8	22.3	47.7	8.37	5.64	51.5
x=80	4.887	70.5	69.8	1.960	1.997	3.54	23.5	8.33	24.6	50.6	9.02	5.27	65.4
x=90	5.073	75.0	69.3	1.980	2.001	3.46	33.2	11.4	26.2	53.1	10.5	4.77	76.2
x=100	5.054	77.7	75.5	1.960	2.001	3.33	23.1	8.25	28.0	57.7	10.2	4.39	84.0

* n_w, n_{3w} : the refractive index at 633nm and 1.9 μm . T_w, T_{3w} : apparent transmittance at 633nm and 1.9 μm . E_g : average excitation energy. E_d : electronic oscillator strength. l_c : coherence length. I/I_{SiO_2} : relative intensity of the third harmonic signal.

grating monochromator and the signal from the photomultiplier detector was stored and processed in a computer. The resolution and the precision of wavenumber are within 1 cm^{-1} . The measured Raman spectra were corrected for thermal population.

^{11}B MAS NMR spectra of powdered glass samples were recorded at 128 MHz on a JEOL JNM-GSX400 MAS FT-NMR spectrometer. A single pulse sequence was used; the pulse length of 0.5–1.0 μs corresponding to a pulse angle of $\sim 22.5^\circ$, the pulse delay of 2.5 s and the accumulation of 16–160 scans. A cylindrical zirconia sample holder was rotated at a speed of about 6 kHz during the ^{11}B MAS NMR measurements. The fraction of 4-coordinated borons (N_4) in Sb_2O_3 - B_2O_3 glasses was determined by integrating the corresponding areas under the ^{11}B NMR spectrum after the peak deconvolution.

The methods to measure the optical absorption spectra, the refractive index, and the THG were described in detail elsewhere.^{10),11)}

3. Results

3.1 IR and Raman spectra

The IR spectra of two crystalline forms of Sb_2O_3 (senarmontite and valentinite) and Sb_2O_3 glass are shown in Fig. 1. The IR band assignment is listed in Table 2. For senarmontite, there is a major peak at 740 cm^{-1} which corresponds to the ν_1 (sym. stretching) vibration mode of SbO_3 trigonal pyramid (tp) with C_{3v} symmetry.⁶⁾ For valentinite, there are four major peaks. The IR bands at 590 and 470 cm^{-1} correspond to the ν_3 (asym. stretching) and ν_4 (asym. bending) vibration modes of SbO_3 tp with C_s or C_1 symmetry, respectively.¹²⁾ The band located at 690 cm^{-1} can be assigned to the ν_1 (sym. stretching) vibration mode and the one at 540 cm^{-1} should be related to the ν_2 (sym. bending) vibration modes.¹³⁾ Bishay and Maghrabi¹⁴⁾ assigned the absorption peak at 940 cm^{-1} for Sb_2O_3 glass to the ν_1 (sym. stretching) vibration mode of SbO_3 . However, this peak was not observed in any Sb_2O_3 -rich glasses, even in

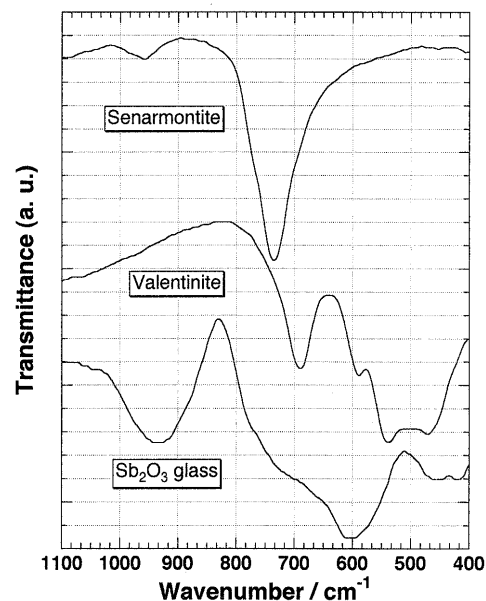


Fig. 1. IR spectra of Sb_2O_3 glass and two crystalline forms, i.e., senarmontite and valentinite.

$90\text{Sb}_2\text{O}_3 \cdot 10\text{B}_2\text{O}_3$ glass, which were melted in Pt-crucible. We, therefore, consider that this peak observed exclusively for Sb_2O_3 glass is due to the Si-O stretching vibration of SiO_4 tetrahedra, which were contaminated from the silica ampoule used for melting Sb_2O_3 .⁶⁾ In fact, using inductively coupled plasma (ICP) we found that the present Sb_2O_3 glass contains 2 mol% of silica. We, therefore, suggest that an IR peak at 960 cm^{-1} observed for senarmontite is due to the combination of the band at 740 cm^{-1} (ν_1 : IR and Raman active) and one of group modes.

We will next deal with the Raman spectra of two crystalline forms of Sb_2O_3 (senarmontite and valentinite) and

Table 2. The Assignments of IR and Raman Spectra of Two Crystalline Forms and Sb_2O_3 Glass
(IR : IR active, R : Raman active, w : weak, s : strong and vs : very strong)

Modes	Senarmontite	Valentinite	Sb_2O_3 glass
$\nu_1(\text{A}_1)$	737 cm^{-1} (R s)	692 cm^{-1} (R s)	700 cm^{-1} (IR s)
	718 cm^{-1} (IR vs)	687 cm^{-1} (IR s)	690 cm^{-1} (R w)
$\nu_2(\text{A}_1)$		541 cm^{-1} (IR s)	
		505 cm^{-1} (R vs)	500 cm^{-1} (R s)
$\nu_3(\text{E})$	592 cm^{-1} (R w)	600 cm^{-1} (R s)	605 cm^{-1} (IR vs)
		591 cm^{-1} (IR s)	600 cm^{-1} (R w)
$\nu_4(\text{E})$	454 cm^{-1} (R vs)	473 cm^{-1} (IR s)	455 cm^{-1} (IR w)
		449 cm^{-1} (R s)	440 cm^{-1} (R vs)
Group modes	377 cm^{-1} (R s)	301 cm^{-1} (R vs)	
	258 cm^{-1} (R vs)	225 cm^{-1} (R s)	240 cm^{-1} (R w)
	193 cm^{-1} (R s)	193 cm^{-1} (R w)	190 cm^{-1} (R w)
	122 cm^{-1} (R w)	149 cm^{-1} (R s)	
		109 cm^{-1} (R w)	

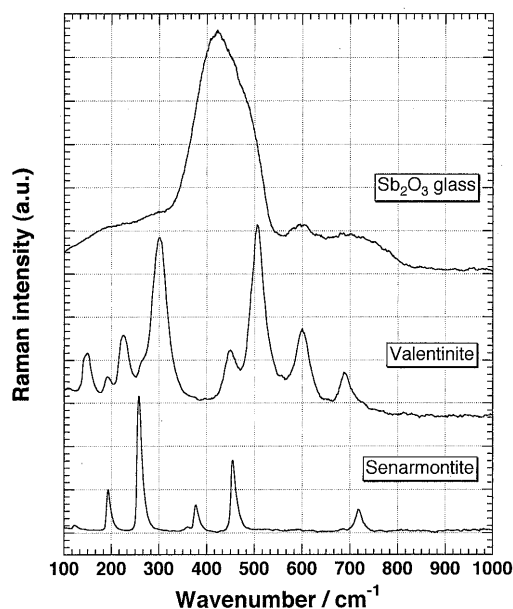


Fig. 2. Raman spectra of Sb_2O_3 glass and two crystalline forms, i.e., senarmontite and valentinite.

Sb_2O_3 glass as depicted in Fig. 2. The band assignment of Raman spectra of senarmontite, valentinite and Sb_2O_3 glass is also listed in Table 2. In this work, we assign the vibrational modes of two crystals and Sb_2O_3 glass on the basis of the molecular spectroscopy of C_{3v} type molecules.¹⁵⁾ The band assignment of this work is, therefore, different from that proposed by Bishay and Maghrabi (i.e., $\nu_1=950$, $\nu_2=600$, $\nu_3=720$ and $\nu_4=465\text{ cm}^{-1}$).¹⁴⁾

The Raman spectra of Sb_2O_3 - B_2O_3 glasses are shown in

Fig. 3. The Raman bands which are typical for borate glasses cannot be seen because of the high Raman scattering intensity of the Sb-O vibration modes. A strong peak at 808 cm^{-1} , which corresponds to the trigonal deformation of oxygen in the boroxol ring,^{16),17)} disappears at 40 mol% Sb_2O_3 . There is a small peak at 770 cm^{-1} in the composition region from 20 to 60 mol% Sb_2O_3 . This peak is assigned to the tetraborate groups which contain BO_4 structural units.¹⁷⁾ So as to interpret these Raman spectra quantitatively, we deconvoluted the bands in the spectral range from 100 to 800 cm^{-1} into six Gaussian peaks. Here, SbO_3 vibration modes are divided into four peaks with reference to valentinite. On the other hand, the group modes, which reflect

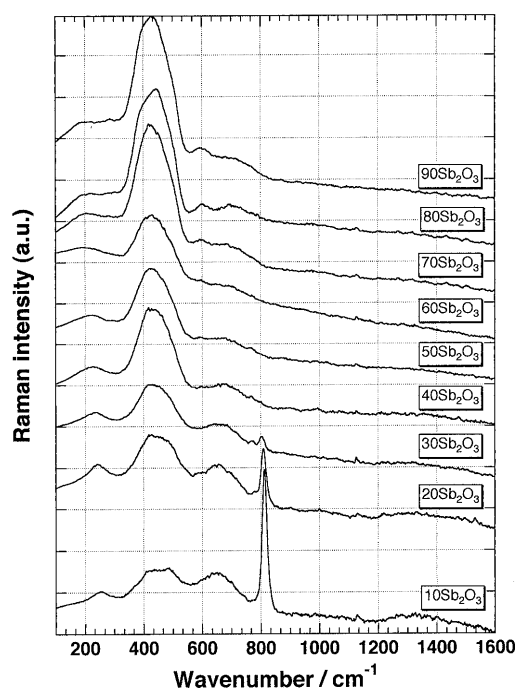


Fig. 3. Raman spectra of Sb_2O_3 - B_2O_3 glasses. The number in each curves denotes the Sb_2O_3 content.

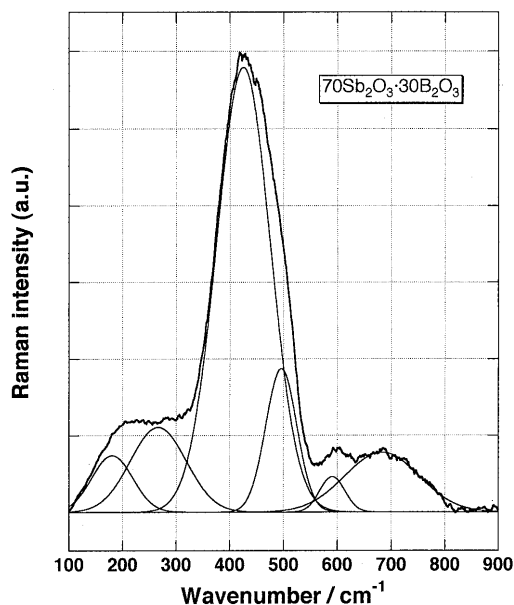


Fig. 4. Peak deconvolution of Raman spectrum of $70\text{Sb}_2\text{O}_3 \cdot 30\text{B}_2\text{O}_3$ glass.

the long range structure, are assumed to be divided into two peaks for convenience. An example of deconvolution for the Raman spectrum of $70\text{Sb}_2\text{O}_3 \cdot 30\text{B}_2\text{O}_3$ glass is shown in Fig. 4. In this figure, weak bands at 690 and 600 cm^{-1} are assigned to the ν_1 (sym. stretching) and ν_3 (asym. stretching) vibration modes of SbO_3 unit, respectively. An intense band near 450 cm^{-1} is divided into two peaks at 500 and 440 cm^{-1} , which are assigned to the ν_2 (sym. bending) and ν_4 (asym. bending) vibration modes of SbO_3 unit, respectively. Peaks at 240 and 190 cm^{-1} correspond to the group modes.^{12),15)}

3.2 ^{11}B MAS NMR spectra

The ^{11}B MAS NMR spectra taken at 128 MHz were used to determine the fraction of BO_4 groups. Figure 5 shows the ^{11}B MAS NMR spectra of $\text{Sb}_2\text{O}_3\text{-B}_2\text{O}_3$ glasses. Although three transitions are possible for the $I=3/2$ spin as in ^{11}B , only the central transition (i.e., $m=+1/2 \leftrightarrow -1/2$) is observed for both the BO_4 and BO_3 groups. This is because the first-order quadrupole interaction broadens the satellite transitions (i.e., $m=+3/2 \leftrightarrow +1/2$ and $m=-1/2 \leftrightarrow -3/2$).¹⁸⁾ A Gaussian peak at 0 ppm is due to BO_4 unit, and the fraction of the BO_4 groups (N_4) in the glasses can be estimated by integrating the peak areas after deconvolution. The obtained N_4 is shown in Fig. 6 as a function of Sb_2O_3 content. We see from Fig. 6 that N_4 value increases with increasing Sb_2O_3 ; it reaches a maximum of 10% at $40\text{ mol}\%$ Sb_2O_3 and finally becomes zero at $90\text{ mol}\%$ Sb_2O_3 . In this figure, the N_4 values of $\text{Bi}_2\text{O}_3\text{-B}_2\text{O}_3$ binary glasses are also appended as a reference.⁵⁾ The N_4 fraction is much smaller for $\text{Sb}_2\text{O}_3\text{-B}_2\text{O}_3$ than for $\text{Bi}_2\text{O}_3\text{-B}_2\text{O}_3$ at all compositions and the latter glasses show its maximum at $30\text{ mol}\%$ Bi_2O_3 . Such a small BO_4 fraction of $\text{Sb}_2\text{O}_3\text{-B}_2\text{O}_3$ glasses relates with the small fraction of tetraborate group as seen in Fig. 3.

3.3 Linear and nonlinear optical properties

Transmittance (T), refractive index (n) and the optical band gap (E_g) are listed in Table 1. The subscripts ω and 3ω correspond to the wavelengths of 1900 and 633 nm , respectively. The refractive index at 1900 nm (n_ω) was obtained from the extrapolation of $1/(n^2-1)$ vs. E^2 plots (E : photon energy) in accordance with Wemple's model.¹⁹⁾

$$\frac{1}{n_\omega^2-1} = \frac{E_0}{E_d} - \frac{E^2}{E_0 E_d} \quad (1)$$

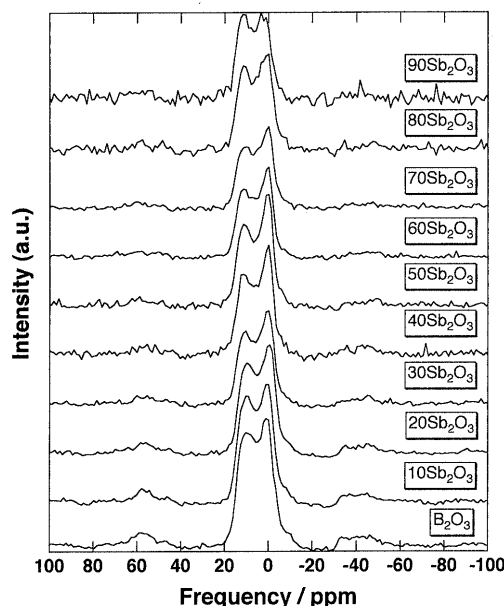


Fig. 5. ^{11}B MAS NMR spectra of $\text{Sb}_2\text{O}_3\text{-B}_2\text{O}_3$ glasses. The number in each spectrum denotes the Sb_2O_3 content.

where E_d is the dispersion energy and E_0 is the oscillator energy. The values of E_d and E_0 are listed in Table 1. In this table, the optical band gap (E_g) of these glasses is also given. The optical band gap was estimated from the extrapolation of $(AE)^2$ vs. E linear plot to the E -axis, where A is the absorption coefficient and E is the photon energy ($h\nu$). The optical band gaps of $\text{Sb}_2\text{O}_3\text{-B}_2\text{O}_3$ glasses are shown in Fig. 7. We notice from Fig. 7 that the optical band gap of B_2O_3 glass abruptly decreases from 7.2 eV to 4.52 eV on addition of only $10\text{ mol}\%$ Sb_2O_3 , gradually decreases with increasing Sb_2O_3 content and then reaches 3.33 eV for Sb_2O_3 glass.

The $\chi^{(3)}$ values obtained are listed in Table 1. The relationship between $\chi^{(3)}$ and the glass composition in $\text{Sb}_2\text{O}_3\text{-B}_2\text{O}_3$ glasses is plotted in Fig. 8, showing that $\chi^{(3)}$ in-

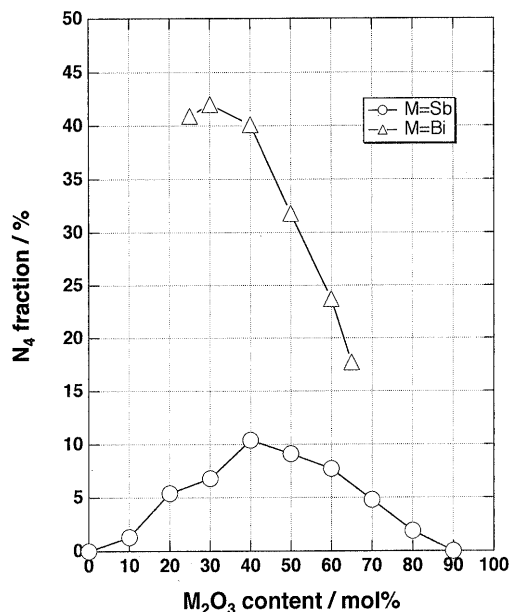


Fig. 6. The fraction of 4-coordinated boron (N_4) as a function of the glass composition for $\text{Sb}_2\text{O}_3\text{-B}_2\text{O}_3$ and $\text{Bi}_2\text{O}_3\text{-B}_2\text{O}_3$ glasses,⁵⁾ which was estimated by ^{11}B MAS NMR spectra.

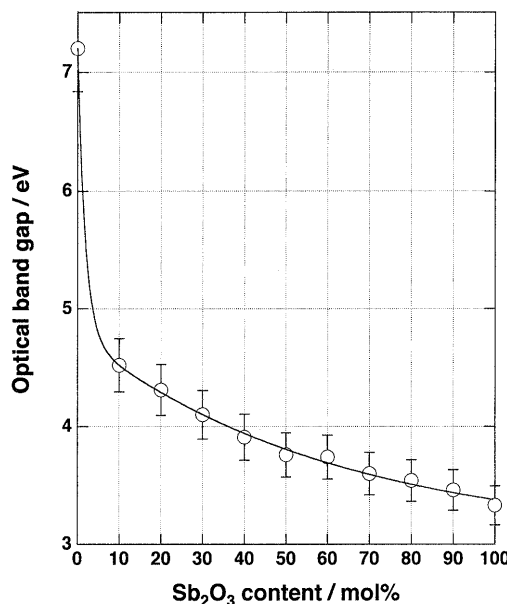


Fig. 7. The optical band gap as a function of the glass composition for $\text{Sb}_2\text{O}_3\text{-B}_2\text{O}_3$ glasses. The solid line is the guide to the eyes.

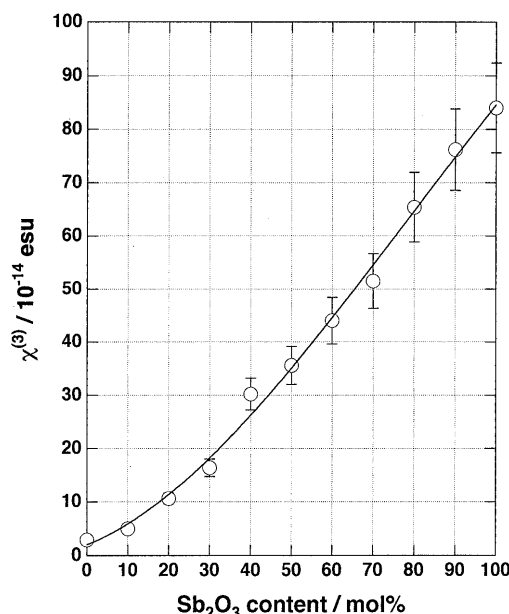


Fig. 8. $\chi^{(3)}$ as a function of the glass composition for Sb_2O_3 - B_2O_3 glasses. The solid line is the guide to the eyes.

creases rapidly with increasing Sb_2O_3 content. The maximal experimental errors in the $\chi^{(3)}$ values are depicted by bars in the figure.

4. Discussion

4.1 Glass structure

4.1.1 Structure of Sb_2O_3 crystals and glass

In general, a glass is known to have a structural unit similar to that in a crystal of the same composition. It is, therefore, useful to know the structure of the corresponding crystals. Sb_2O_3 exists in two forms, the cubic form, senarmonite, which is stable below 570°C and the orthorhombic form, valentinite, which is stable above this temperature and melts at 656°C. Senarmonite has a structure consisting of the Sb_4O_6 molecules, namely, the SbO_3 pyramids being linked at their corners to form a cage-like structure.²⁰⁾ The valence angle of SbO_3 is 109.28° and the Sb-O distance is 0.20 nm.²¹⁾ Valentinite also consists of SbO_3 pyramids but has a double chain structure consisting of four-membered rings of SbO_3 pyramids.²⁰⁾ The SbO_3 pyramids are deformed considerably from a regular tetrahedral shape, that is, the valence angles of SbO_3 are 81, 93 and 99° and the Sb-O distance ranges from 0.198 to 0.202 nm.²²⁾

The structure of Sb_2O_3 glass was investigated by X-ray diffraction analysis by Imaoka et al.²⁰⁾ They proposed that the network structure of the glass is a double chain consisting of four-membered rings of SbO_3 pyramids as found in the orthorhombic form of Sb_2O_3 valentinite on the basis of the fact that the average the valence angle of SbO_3 is about 92° and the Sb-O distance is 0.199 nm. In this case, the valence angles of SbO_3 pyramid are much less than the tetrahedral angle (109.5°), indicating that the Sb-O bonds in both valentinite crystal and Sb_2O_3 glass are rich in *p*-character and the lone pair electrons are rich in *s*-character. In the following, we will discuss the structure of Sb_2O_3 glass by comparing the vibrational spectra of the crystalline Sb_2O_3 with those of Sb_2O_3 glass.

As seen from Figs. 1 and 2, the IR and Raman bands of Sb_2O_3 glass are interpreted in terms of the vibration modes of valentinite. For valentinite and Sb_2O_3 glass, both ν_3 (asym. stretching) and ν_4 (asym. bending) vibration modes are split into two peaks, which indicates that the SbO_3 unit

belongs not to C_{3v} but to C_s or C_1 symmetry groups.¹⁵⁾ Such symmetry lowering means that the SbO_3 unit of Sb_2O_3 glass does not form a cage-like structure of Sb_4O_6 as found in senarmonite, but the network structure of Sb_2O_3 glass is similar to valentinite which consists of double-chain structure of SbO_3 unit as mentioned by Imaoka et al.⁸⁾

4.1.2 Structure of Sb_2O_3 - B_2O_3 binary glasses

In the previous section, we discussed the structure of Sb_2O_3 glass. Our interest here is how the network structure of Sb_2O_3 - B_2O_3 glasses changes with the composition. The IR spectroscopic investigation on the Sb_2O_3 - B_2O_3 glass was carried out by Mochida and Takahashi.⁶⁾ They concluded that Sb^{3+} ions exist as SbO_3 pyramids due to the covalent character of Sb-O bonds. Recently, Zubkova et al.⁷⁾ have made the Raman spectroscopic study of Sb_2O_3 - B_2O_3 glasses and proposed that the composition dependent regularities in the Raman spectra and physicochemical properties of glasses can be satisfactorily explained if the formation of two stable structural groups is assumed, i.e., $\text{Sb}_2\text{O}_3 \cdot 4\text{B}_2\text{O}_3$ and $2\text{Sb}_2\text{O}_3 \cdot 3\text{B}_2\text{O}_3$.

In this study, the Raman spectra of the present glass system were investigated, and the bands of Sb_2O_3 - B_2O_3 glasses are assigned and deconvoluted with reference to six vibrational modes of valentinite form as seen in Fig. 3 and Table 2. As in Fig. 3, the boroxol ring disappears at more than 40 mol% Sb_2O_3 . This result indicates the cleavage of the three-membered boroxol ring by the introduction of Sb^{3+} ions. However, the tetraborate group, which appears in place of boroxol group and contains one BO_4 unit, is relatively small. There are no other peaks which suggest the presence of borate groups other than boroxol and tetraborate groups. Here, we further take a look at the structure of Sb_2O_3 - B_2O_3 glasses on the basis of the ^{11}B MAS NMR spectroscopic study.

As seen in Fig. 6, comparing trivalent cations, the fraction of BO_4 unit is much smaller for Sb_2O_3 - B_2O_3 than for Bi_2O_3 - B_2O_3 glasses at all compositions. Furthermore, the N_4 for Bi_2O_3 - B_2O_3 glasses reaches its maximal faster than that for Sb_2O_3 - B_2O_3 glasses. These results indicate that the oxygen-donation of metal oxide to BO_3 and the formation of the non-bridging oxygen is much smaller for Sb_2O_3 - B_2O_3 than for Bi_2O_3 - B_2O_3 .

If all antimony ions exist as trivalent cations and are 3-coordinated, the corresponding boron ions should remain 3-coordinated. As in Fig. 6, however, the formation of 4-coordinated boron has been confirmed, although the fraction of BO_4 is as small as 10% at 40 mol% Sb_2O_3 . According to the chemical analysis,⁸⁾ the fraction of Sb^{5+} in the Sb_2O_3 - B_2O_3 glasses is less than 2.0 mass% and is not enough to compensate negative charge of BO_4^- . This result may be explained by considering the existence of 3-coordinated oxygen as suggested by Miyaji et al.²³⁾ for PbO - Ga_2O_3 and Bi_2O_3 - Ga_2O_3 glasses. That is, the 3-coordinated boron may further be coordinated by the bridging oxygen in the Sb-O-Sb bond, resulting in the formation of 4-coordinated boron. The formation of BO_4 in the tetraborate group can be explained by this mechanism. However, such an assumption of three coordinated oxygen is clearly contradict to Zachariasen's rule. It should be ascertained, for example, by using ^{17}O double rotation (DOR) NMR spectroscopy.

In short, it is considered that, in borate glasses, SbO_3 unit mainly acts as a network former even at low Sb_2O_3 contents to form network structure through Sb-O-B bonds. Such an attitude as a network former of Sb_2O_3 is ascribed to the tightly-bound covalent character of Sb-O bonds, which is reflected in the small N_4 fraction of Sb_2O_3 - B_2O_3 glasses.

4.2 $\chi^{(3)}$ from the point of the optical band gap

It was concluded that the coordination around Sb^{3+} ion does not change with the composition for Sb_2O_3 - B_2O_3 glass-

es. In this section, we discuss the optical nonlinearity in terms of the optical band gap to understand the effect of hybridization of Sb^{3+} ion on the nonlinear optical properties of glasses.

The color of $\text{Sb}_2\text{O}_3\text{-B}_2\text{O}_3$ glasses turns from colorless to pale-yellow as the Sb_2O_3 content becomes high. This change corresponds to the fact that the optical band gap (E_g) between HOMO ($\text{Sb } 5s + \text{O } 2p_\pi$) and LUMO ($\text{Sb } 5p$) become small. The decrease in optical band gap in the present glasses (see Fig. 7) is considered to arise from the following reason. Because of the overlap of $\text{Sb } 5s$ and $\text{O } 2p_\pi$ accompanied by lowering of the energy level of $\text{Sb } 5p$ down to the band gap, the increase in covalency and decrease in optical band gap occur,^{24),25)} as stated in the previous Section (see Section 4.1.1). The monotonous decrease of the optical band gap indicates that no significant structural change occurs in the present glasses. Such a decrease in the optical band gap plays a main role in the enhancement of $\chi^{(3)}$ as will be described below.

As previously reported by Hashimoto and Yoko,²⁶⁾ the $\chi^{(3)}$ of transition metal oxides (TMOs) with small optical band gap such as $\alpha\text{-Fe}_2\text{O}_3$ and V_2O_5 , was 10^{-12} – 10^{-11} esu, which is higher than that of SiO_2 by 2–3 orders of magnitude. This is ascribed to the small optical band gap of TMOs because the band gap model^{26),27)} predicts that a material with a small optical band gap (E_g) shows a high $\chi^{(3)}$. According to this model, it is hence expected that an enhancement of $\chi^{(3)}$ occurs when a frequency of interacting light approaches either one, two, or three-photon resonance.^{26),27)}

$$\chi^{(3)} = \frac{\Phi}{(E_g - 3\omega) \cdot (E_g - 2\omega) \cdot (E_g - \omega)} \quad (2)$$

where Φ is a phenomenological parameter. The solid line shown in Fig. 9 indicates the value of $\chi^{(3)}$ predicted by Eq. (2). It is clear that $\chi^{(3)}$ increases asymptotically as the optical band gap approaches the three-photon energy, namely, 1.96 eV. The observed points deviate to a considerable extent from the values predicted by Eq. (2) when the optical band gap is small. This may be ascribed to the pre-resonance effect which involves the enhancement of the

transition moment.^{10),11)}

As indicated in the Section 4.1.1, the $5s$ -orbital of the Sb^{3+} ion in Sb_2O_3 , unlike other p -block elements such as PbO and Bi_2O_3 ,²⁴⁾ is fairly localized as the lone pair and is not delocalized by the coordination of oxygen. Such a localized HOMO level is expected to have fairly large density of state (DOS). The higher DOS around the top of the valence band give rise to the higher optical transition probability and furthermore the larger $\chi^{(3)}$. Further theoretical investigation is needed for the band structure Sb_2O_3 glass.

4.3 $\chi^{(3)}$ on the basis of Lines' bond orbital theory

We investigated the $\chi^{(3)}$ dependence on the optical band gap. Such a band gap model does not hold well for the present glass system. In order to investigate the relationship between $\chi^{(3)}$ and the linear optical properties, we next introduce Lines' bond orbital theory.²⁸⁾ According to this theory, the $\chi^{(3)}$ value is expressed by using measurable properties (i.e., n_ω , E_0 and the bond length). This formula implies that $\chi^{(3)}$ value is proportional to the term $(n_\omega^2 + 2)^3 \cdot (n_\omega^2 - 1) \cdot d^2 / E_0^2$ at frequencies corresponding to $(\hbar\nu)^2 \ll E_s^2$. It has been found that the $\chi^{(3)}$ value estimated from this term is in good agreement with the experimental value for TeO_2 glass.²⁹⁾ However, this cannot be applied to the present binary glasses because it is difficult to evaluate experimentally the proper M–O bond length (d) for these glasses. This problem may be solved by using Wemple's single oscillator approximation ($E_d \propto d^2$).^{25),30)} By substituting E_d for d^2 , $\chi^{(3)}$ can be expressed as follows.³⁰⁾ Hereafter, we call this relationship "modified Lines' equation".

$$\chi^{(3)} \propto (n_\omega^2 + 2)^3 \cdot (n_\omega^2 - 1) \cdot \frac{E_d}{E_0^2} \quad (3)$$

So far, this relationship has been found to be useful to calculate the theoretical $\chi^{(3)}$ qualitatively and to search the material with high $\chi^{(3)}$.^{5),11),30)} Figure 10 shows the relationship between $\chi^{(3)}$ and $(n_\omega^2 + 2)^3 \cdot (n_\omega^2 - 1) \cdot E_d / E_0^2$ in $\text{Sb}_2\text{O}_3\text{-B}_2\text{O}_3$ glasses. It seems that this theory can predict rather well observed points. This relation is considered to be of great significance because it is possible to predict the $\chi^{(3)}$ value from the three optical parameters, n_ω , E_d and E_0 determined experimentally with an ellipsometry.

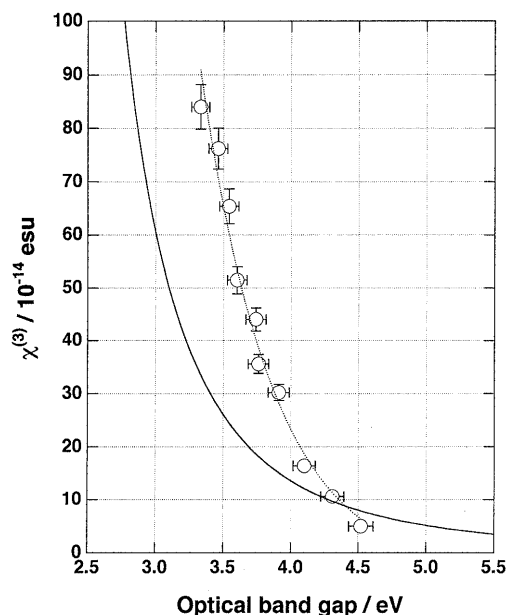


Fig. 9. $\chi^{(3)}$ as a function of the optical band gap in $\text{Sb}_2\text{O}_3\text{-B}_2\text{O}_3$ glasses. The solid line is the curve based on Eq. (2). The dotted line is the guide to the eyes.

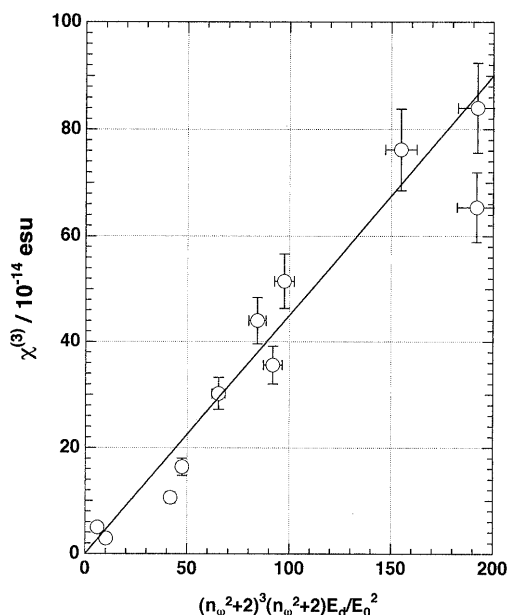


Fig. 10. $\chi^{(3)}$ as a function of the modified Lines' parameter $(n_\omega^2 + 2)^3 \cdot (n_\omega^2 - 1) \cdot E_d / E_0^2$ for $\text{Sb}_2\text{O}_3\text{-B}_2\text{O}_3$ glasses. The solid line is the fitting line.

5. Conclusion

The third order nonlinear optical susceptibilities $\chi^{(3)}$ of $\text{Sb}_2\text{O}_3\text{-B}_2\text{O}_3$ binary glasses have been investigated by the third harmonic generation (THG) method. The structure of the glasses has been also discussed on the basis of IR, Raman and ^{11}B MAS NMR spectra. The conclusions are as follows.

(1) The IR and Raman spectroscopic study indicated that the structure of Sb_2O_3 glass is similar to that of valentinite which consists of double-chains of SbO_3 units, not to that of senarmontite.

(2) The formation of 4-coordinated boron is much smaller for $\text{Sb}_2\text{O}_3\text{-B}_2\text{O}_3$ glasses than for $\text{Bi}_2\text{O}_3\text{-B}_2\text{O}_3$ glasses at all compositions, which is due to the covalent character of Sb-O bonds.

(3) In the present glasses, Sb_2O_3 is present as SbO_3 trigonal pyramid even at low Sb_2O_3 composition and takes part in the network formation through Sb-O-B bond.

(4) $\chi^{(3)}$ of $\text{Sb}_2\text{O}_3\text{-B}_2\text{O}_3$ glasses increases with increasing content of Sb_2O_3 with a covalent bond. Especially for Sb_2O_3 glass, $\chi^{(3)}$ value is 8.4×10^{-13} esu, which is about 30 times larger than SiO_2 glass.

(5) $\chi^{(3)}$ was found to change almost linearly with the modified Lines' term for $\text{Sb}_2\text{O}_3\text{-B}_2\text{O}_3$ binary glasses.

Acknowledgment This work was supported by a Grant-in Aid for Scientific Research from the Ministry of Education, Science and Culture, Japan. One of the authors (T.Y.) would like to thank The Iketani Science and Technology Foundation for the partial financial support to this work. Special thanks are given to Dr. S. Hayakawa at Okayama University for helping with ^{11}B MAS NMR measurements and helpful comments.

References

- 1) R. Adair, L. L. Chase and S. A. Payne, *J. Opt. Soc. Am. B*, **4**, 875-81 (1987).
- 2) D. W. Hall, M. A. Newhouse, N. F. Borrelli, W. H. Dombaugh and D. L. Weidman, *Appl. Phys. Lett.*, **54**, 1293-95 (1989).
- 3) K. Fajans and N. Kreidl, *J. Am. Ceram. Soc.*, **31**, 105-14 (1948).
- 4) J. R. Tessman, A. H. Kahn and W. Shockley, *Phys. Rev.*, **92**, 890-95 (1953).
- 5) K. Terashima, T. Hashimoto and T. Yoko, accepted to *Phys. Chem. Glasses* (1996).
- 6) N. Mochida and K. Takahashi, *Yogyo-Kyokai-Shi*, **84**, 413-20 (1976).
- 7) L. V. Zubkova, M. M. Pivovarov and O. V. Yanush, *Glass Phys. Chem.*, **20**, 23-32 (1994).
- 8) M. Imaoka, H. Hasegawa and S. Shindo, *Yogyo-Kyokai-Shi*, **77**, 263-71 (1969).
- 9) V. V. Golubkov and M. M. Pivovarov, *Fiz. Khim. Stekla*, **17**, 253-60 (1991).
- 10) K. Terashima, S. H. Kim and T. Yoko, *J. Am. Ceram. Soc.*, **78**, 1601-05 (1995).
- 11) K. Terashima, T. Hashimoto and T. Yoko, *Phys. Chem. Glasses*, **37**, 129-33 (1996).
- 12) P. J. Miller and C. A. Cody, *Spectrochim. Acta*, **38A**, 555-59 (1982).
- 13) I. L. Botto, E. J. Baran, C. Cascales, I. Rasines and R. S. Puche, *J. Phys. Chem. Solids*, **52**, 431-34 (1991).
- 14) A. Bishay and C. Maghrabi, *Phys. Chem. Glasses*, **10**, 1-12 (1969).
- 15) K. Nakamoto, "Infrared and Raman Spectra of Inorganic and Coordination Compounds, 4th ed.", John Wiley & Sons, New York (1986) pp. 115-25.
- 16) J. Krogh-Moe, *Phys. Chem. Glasses*, **6**, 46-54 (1965).
- 17) B. N. Meera and J. Ramakrishna, *J. Non-Cryst. Solids*, **159**, 1-21 (1993).
- 18) P. J. Bray, *J. Non-Cryst. Solids*, **95-96**, 45-60 (1987).
- 19) S. H. Wemple, *Phys. Rev. B*, **7**, 3767-77 (1973).
- 20) H. Hasegawa, M. Sone and M. Imaoka, *Phys. Chem. Glasses*, **19**, 28-33 (1978).
- 21) C. Svensson, *Acta Cryst.*, **B31**, 2016-18 (1975).
- 22) C. Svensson, *Acta Cryst.*, **B30**, 458-61 (1974).
- 23) F. Miyaji, T. Yoko, J. Jin, S. Sakka, T. Fukunaga and M. Misawa, *J. Non-Cryst. Solids*, **175**, 211-23 (1994).
- 24) J. A. Duffy and G. O. Kyd, *Phys. Chem. Glasses*, **36**, 101-05 (1995).
- 25) S. H. Wemple, *J. Chem. Phys.*, **67**, 2151-68 (1977).
- 26) T. Hashimoto and T. Yoko, *Appl. Optics*, **34**, 2941-48 (1995).
- 27) F. Kajzar, J. Messier and C. Rosillio, *J. Appl. Phys.*, **60**, 3040-44 (1986).
- 28) M. E. Lines, *Phys. Rev. B*, **41**, 3372-90 (1990).
- 29) S. H. Kim, T. Yoko and S. Sakka, *J. Am. Ceram. Soc.*, **76**, 2486-90 (1993).
- 30) S. H. Kim and T. Yoko, *J. Am. Ceram. Soc.*, **78**, 1061-65 (1995).